Journal of Physics G: Nuclear and Particle Physics

PAPER

Clusterization in low and intermediate density nuclear matter in the modified nuclear statistical equilibrium model

To cite this article: Rula Bakeer *et al* 2019 *J. Phys. G: Nucl. Part. Phys.* **46** 025105

View the article online for updates and enhancements.

You may also like

- Nuclei in central engine of core-collapse supernovae
Shun Furusawa
- Equation-of-state Table with Hyperon and Antikaon for Supernova and Neutron Star Merger
Tuhin Malik, Sarmistha Banik and Debades Bandyopadhyay
- Equilibrium constants of hydrogen and helium isotopes at low nuclear densities
R Bougault, E Bonnet, B Borderie et al.

This content was downloaded from IP address 176.119.249.5 on 08/04/2023 at 08:55

IOP Publishing Journal of Physics G: Nuclear and Particle Physics

J. Phys. G: Nucl. Part. Phys. **46** (2019) 025105 (13pp) https://doi.org/10.1088/1361-6471/aaf95b

Clusterization in low and intermediate density nuclear matter in the modified nuclear statistical equilibrium model

Rula Bakeer, Waad Awad and H R Jaqaman

Department of Physics, Birzeit University, Birzeit, Palestine

E-mail: hjaqaman@birzeit.edu

Received 6 September 2018, revised 26 November 2018
Accepted for publication 14 December 2018
Published 15 January 2019

Abstract.
The formation of light and intermediate clusters in low and intermediate density nuclear matter is investigated within the modified nuclear statistical equilibrium model. We include clusters up to mass number $A = 61$ and densities up to 0.1 nucleons fm^{-3}. The original nuclear statistical equilibrium model is modified by using density-dependent cluster binding energies. Whereas the light clusters are dominant at very low densities, it is found that the intermediate clusters become dominant at higher densities. As the temperature increases the dominance of the lighter clusters grows at the expense of the heavier clusters. We also evaluate the equation of state of nuclear matter within this model and determine that the critical temperature is 12.5 MeV, well below the values predicted by other equations of state. Finally we calculate the fragment multiplicity distribution within this model and find that its derivative $\frac{dM}{dT}$ has a maximum at a temperature (the liquid–gas transition temperature) close to that expected by other calculations.

Keywords: nuclear matter, nuclear statistical equilibrium model, nuclear equation of state, multiplicity derivitive

1. Introduction

The abundance of light clusters in nuclear matter at very low densities and moderate temperatures has been the subject of several theoretical [1–6] and experimental [7, 8] investigations. The light clusters are abundant only at very low densities because their binding energy decreases as the density increases and they finally dissolve above a certain critical density (the Mott density) [9] where their binding energy goes to zero. With the dissolution of

 © 2019 IOP Publishing Ltd Printed in the UK

the light clusters, the intermediate mass fragments become dominant at the higher densities because of their higher Mott densities until nuclear matter becomes homogeneous again as it approaches saturation density. This dominance of the intermediate mass fragments at the higher densities has been observed experimentally [10] and has been predicted theoretically in the statistical multifragmentation models [11–14]. The aim of the present work is to investigate the abundance of intermediate mass clusters in low density nuclear matter (hereafter referred to as the vapour) within a modified version of the nuclear statistical equilibrium model (NSE).

In an earlier work [6] the formation of light clusters ($A \leqslant 4$) at very low nuclear matter densities was investigated within a modified version of the NSE model. The original NSE model [15–17] assumes that each cluster is in thermal and chemical equilibrium with the surrounding free nucleons comprising the surrounding vapour. It also assumes that a cluster has the same binding energy as the equivalent isolated nucleus with the same charge and mass number. This last assumption is valid only at extremely low densities of the surrounding vapour (less than 10^{-2} nucleons fm^{-3}) and so the model breaks down at higher densities.

In the modified NSE model employed here the cluster's binding energy is allowed to vary with the density of the surrounding medium in order to reflect the effect of Pauli blocking. This effect arises from the indistinguishability between the nucleons inside the clusters and the free nucleons in the surrounding vapour. In an earlier work [6] the formation of light clusters was found to have a noticeable effect on the equation of state of nuclear matter in the vapour state. Similar effects on the equation of state of the vapour were obtained even when only alpha clusters are included [18]. Clustering was also found to reduce the critical temperature of infinite nuclear matter by about 2.4 MeV [1]. The change in the equation of state of nuclear matter was also found [6] to cause a lowering of the limiting temperature which is the highest temperature at which a hot nucleus can survive while in equilibrium with the surrounding vapour. Above the limiting temperature the hot nucleus is unstable because of the Coulomb force [19, 20].

In the following sections we will describe the NSE model and its modification, and then use it to calculate the abundance of the various clusters up to $A = 61$ in nuclear matter at low and intermediate densities up to 0.1 nucleons fm^{-3}. We will then evaluate the resulting nuclear equation of state and determine the critical temperature for the liquid–gas phase transition. We will also evaluate the cluster multiplicity to be expected in a system with a finite number of nucleons using the cluster abundances obtained in the present model.

2. The NSE model and its modification

The NSE model assumes that the free nucleons interact only by forming clusters with which they are in thermal and chemical equilibrium. This is achieved by relating the chemical potential μ_C of cluster type C (containing Z protons and N neutrons) to the chemical potentials of the free nucleons by the relation:

$$\mu_C = Z\mu_P + N\mu_n = A\mu_{\mathrm{id}}, \tag{1}$$

where the last equality follows from treating the protons (p) and neutrons (n) equally in symmetric nuclear matter with the Coulomb force switched off and μ_{id} is the chemical potential of the free nucleons which are treated as an ideal Fermi gas at a temperature T (in MeV). The expression for μ_{id} was derived in [21] and used in [6]:

$$\mu_{\rm id}(T,\,\rho_{\rm free}) = T\left[\ln\left[\frac{\lambda_T^3\rho_{\rm free}}{g}\right] + \sum_{n=1}^{\infty} b_n \frac{n+1}{n}\left[\frac{\lambda_T^3\rho_{\rm free}}{g}\right]^n\right], \tag{2}$$

where $\rho_{\rm free}$ is the density of the free nucleons, $g = 4$ is the nucleon's spin-isospin degeneracy factor, $\lambda_T = \left(\frac{2\pi\hbar^2}{mT}\right)^{1/2}$ is the nucleon's thermal wavelength and the b_n coefficients are listed in [6] up to $n = 6$. The summation in equation (2) converges rapidly and no $n > 6$ coefficients are needed for the densities considered here.

The partial density of each type of cluster is then determined by the equation:

$$\rho_C = \frac{g_C}{(2\pi)^3}\int {\rm d}^3k\ \{\exp\left[(\varepsilon_C^0 - \mu_C - B_C)/T\right] \pm 1\}^{-1}\,, \tag{3}$$

where the (+) and the (−) signs are used for the fermionic and bosonic clusters, respectively, and where g_C, ε_C^0 and B_C are, respectively, the spin degeneracy factor, kinetic energy and binding energy of cluster C.

The NSE model however ignores the reduction in the binding energy of the clusters as the density of the surrounding medium increases which ultimately leads to the dissolution of the clusters at the Mott density. The decrease in the binding energy is due to the Pauli blocking effect mentioned above and its linear dependence on the density follows from the Hartree–Fock approximation [1, 3]. It must be noted that an empirical quadratic term is added in [3] to the Hartree–Fock term but the deviation from linearity is small.

To remedy this deficiency of the model we use in equation (3) cluster binding energies that decrease linearly with total density of the surrounding medium and vanish at each cluster's Mott density:

$$B_C = B_C^0\left(1 - \frac{\rho}{\rho_M(A_C,\,T)}\right) = B_C^0 - \alpha\rho. \tag{4}$$

In equation (4) B_C is the binding energy of cluster C of mass number A_C when immersed in nuclear matter of total density ρ, B_C^0 is the binding energy of the corresponding isolated nucleus of mass number A_C, $\rho_M(A_C,\,T)$ is the Mott density of cluster C at temperature T. The Mott density is related to the slope parameter α in equation (4) by the equation:

$$\rho_M(A_C,\,T) = B_C^0/\alpha. \tag{5}$$

The total density ρ of nuclear matter is the sum of the densities of the free nucleons and the partial densities of the various clusters and is given by:

$$\rho = \rho_{\rm free} + \sum_C A_C\,\rho_C. \tag{6}$$

Unfortunately however there is very little available information about the Mott densities of clusters with $A > 4$ (see e.g. [22]). The situation is somewhat better for the case of the light clusters $A \leqslant 4$ where there is some theoretical [3] and experimental [23] information about the values of the Mott densities. In the present work we adopt the values of the Mott densities for the light clusters $A = 2$, 3 and 4 of Typel *et al* [3] which were obtained with the use of relativistic mean field theory for several temperatures in the range 0–20 MeV. These Mott densities, for a given cluster, are first interpolated as a function of temperature by a simple quadratic polynomial in T and then, for each desired temperature, they are fitted as a function of mass number by a quadratic polynomial in A of the form:

Table 1. Values of the quadratic polynomial coefficients (in fm^{-3}) for the Mott densities $\rho_M(A,\ T)$ at different temperatures T (in MeV).

T	$p(T)$	$q(T)$	$r(T)$
2	0.0012	−0.0049	0.0062
4	0.001 45	−0.0061	0.0085
6	0.0016	−0.006 65	0.0098
8	0.001 75	−0.007 25	0.0113
10	0.0019	−0.007 75	0.0126
12	0.0021	−0.0086	0.0145

$$\rho_M(A,\ T) = p(T)A^2 + q(T)A + r(T) \tag{7}$$

and then extrapolated to $A > 4$. The values of the coefficients in equation (7) obtained in this way are summarized in table 1. Since the present calculations are limited to densities up to 0.1 fm^{-3}, it is seen from the values listed in table 1 that for A larger than about 10 the Mott densities are larger than 0.1 fm^{-3} and so the results should not be very sensitive to them.

The motivation for using the quadratic dependence on the mass number A in equation (7) can be seen by examining equation (5). If we ignore for the moment the A dependence of the slope parameter α then the Mott density should have the same A dependence as the binding energy B_C^0 of the corresponding isolated nucleus. It is well known that the binding energy per particle of light nuclei up to about mass 10 increases on the average linearly with the mass number so that B_C^0 is approximately a quadratic function in A. Of course the slope parameter also increases with A as can be seen from examining the results of Typel *et al* [3] but this A dependence can be absorbed by renormalizing the coefficients of the quadratic polynomial. Along the same line higher order terms may be needed for heavier nuclei but since we have only the Mott densities for $A = 2$, 3 and 4 no higher order terms can be determined from the currently available information.

Since the cluster binding energies depend on the total density and hence on the cluster partial densities and the calculation of the cluster partial densities depends on the binding energies, equations (3), (4) and (6) are solved iteratively until self-consistency is achieved and the abundance of the various clusters is determined to an accuracy of 2% at each given temperature and for each total density.

One problem that arises in the NSE model is the overestimation of the deuteron abundance. This problem has been studied in [3, 24] and is due to the strength of the two-body correlations and the deuteron's small binding energy so that deuteron-like clusters are easily formed. We follow Röpke's suggestion [24] to avoid this overestimation by limiting the integration in equation (3) for the case of the deuteron to momenta $k > k_d^{\mathrm{Mott}}$ where the Mott momentum k_d^{Mott} is defined in [24].

3. The cluster abundances

The calculations for the cluster abundances in symmetric nuclear matter as a function of density and temperature were carried out by including 128 different clusters with $2 \leqslant A \leqslant 61$. The upper mass limit was chosen to ensure that the most stable nuclei in the iron region are included in the calculation. As it turned out however, the heaviest clusters have a significant contribution only at the lowest temperatures as will be seen below. For each mass number A the most stable isolated isobar was chosen as well as any other isobar whose

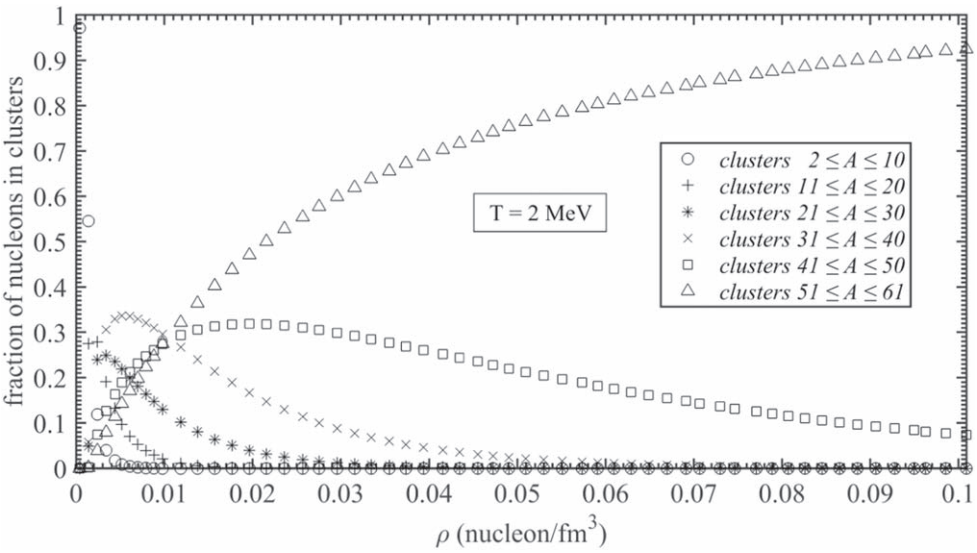

Figure 1. Cluster abundances at $T = 2$ MeV as a function of the total density.

binding energy per nucleon differed from that for the most stable isobar by less than 0.1 MeV. According to these criteria 39 nuclides were chosen with $51 \leqslant A \leqslant 61$ and 32 different nuclides were chosen with $41 \leqslant A \leqslant 50$.

The results for symmetric nuclear matter at $T = 2$ MeV are shown in figure 1 where the clusters are divided by size into six groups. The abundance of any cluster type (of mass number A and charge number Z) at a particular density is defined as the fraction of nucleons at that density that are bound in clusters of that type. The sum of all the cluster abundances when added to the abundance of the free nucleons must be 1 as expected from equation (5). At extremely low densities (less than 0.001 nucleons fm^{-3}) we see that the lightest clusters $2 \leqslant A \leqslant 10$ are dominant but their abundance drops rapidly and becomes negligibly small for higher densities. This is mainly due to their extremely low Mott densities at this temperature. The heavier clusters start to become more abundant at increasingly higher densities with the clusters $31 \leqslant A \leqslant 40$ being dominant for $0.003\ \mathrm{fm}^{-3} < \rho < 0.01\ \mathrm{fm}^{-3}$ and with the still heavier clusters $A > 40$ dominating for higher densities. For the highest density range $0.06\ \mathrm{fm}^{-3} < \rho < 0.1\ \mathrm{fm}^{-3}$ the abundance of the group of heaviest clusters $51 \leqslant A \leqslant 61$ exceeds 80%. However since, as mentioned above, this group contains 39 different cluster types the contribution of each cluster type is about 2% only. The dominance of the heavy fragments at $T = 2$ MeV can be easily understood if we think of these 'relatively cold' nuclei as liquid drops remaining intact and in equilibrium with a very dilute vapour of nucleons and light clusters.

At $T = 2$ MeV the lightest clusters $2 \leqslant A \leqslant 10$ are mostly α particles whereas at higher temperatures the lightest clusters are mostly deuterons. This can be seen by examining figure 2 which gives the abundance of deuterons and alphas at $T = 2$, 3 and 4 MeV. At $T = 2$ MeV and low densities $\rho < 0.001\ \mathrm{fm}^{-3}$ the alpha particles are dominant with a small presence of deuterons. This dominance of the alphas over the deuterons at $T = 2$ MeV is also predicted in [3]. The dominance of the alpha particles at this low temperature can be attributed to their high binding energy. At $T = 2$ MeV the nucleons bound in alphas and deuterons account for about 90% of nuclear matter at low densities while the free nucleons and all the

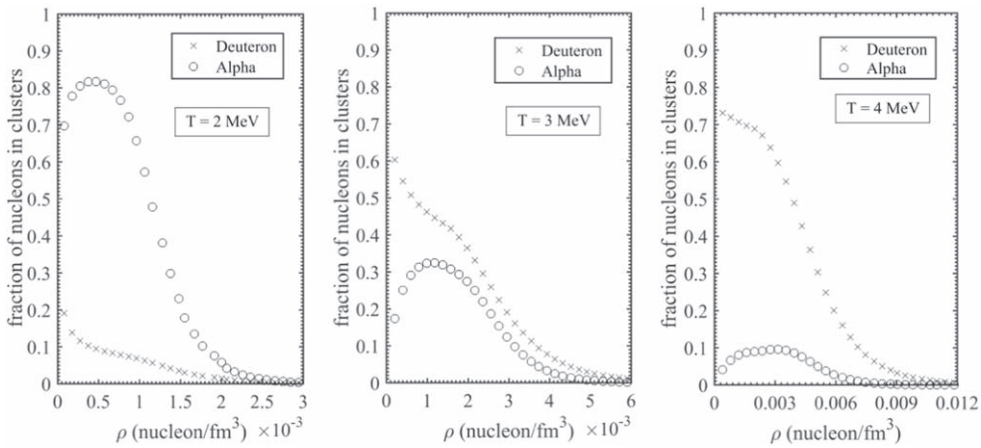

Figure 2. Deuteron and alpha cluster abundances in symmetric nuclear matter at $T = 2$, 3 and 4 MeV as a function of the total density.

other clusters in the range $A \leqslant 10$ have a combined total contribution of only about 10%. It must be noted that above $\rho = 0.001$ fm^{-3} the total contribution of the whole group of lightest clusters $2 \leqslant A \leqslant 10$ is negligible anyway.

At $T = 3$ MeV the deuterons and alphas are present with almost equal contributions, except at the lowest densities where the number of nucleons bound in deuteron clusters is twice to three times the number of those bound in alpha clusters as can be seen from the middle graph in figure 2. At the higher temperature $T = 4$ MeV only deuterons have a significant contribution with the alphas having a much smaller contribution. The dominance of the deuterons for $T \geqslant 4$ MeV at low densities can be attributed to the strength of the two-body correlations whereas at higher densities many-body correlations play an increasingly more important role.

At the higher temperature $T = 4$ MeV the cluster abundances in symmetric nuclear matter undergo a noticeable change as compared with those at $T = 2$ MeV as can be seen in figure 3. Due to their higher Mott densities at this temperature, the lightest clusters (now mostly deuterons as noted above) dominate up to 0.01 fm^{-3} and survive to about twice that density. For higher densities the next heavier group $11 \leqslant A \leqslant 20$ dominates up to 0.025 nucleons fm^{-3}, then the clusters in the range $21 \leqslant A \leqslant 30$ dominate up to a total density of 0.035 fm-3 and so on. The most dramatic change from the lower temperature is that the abundance of the heaviest set of clusters $51 \leqslant A \leqslant 61$ no longer dominates at any density and actually their contribution does not exceed 38% at the highest density considered. This can be understood within the liquid–gas phase transition model with the hot heavy clusters losing mass by evaporation and fragmentation and their slightly smaller remnants coexisting with the surrounding vapor of nucleons and light clusters.

Figure 4 shows the various cluster abundances for symmetric nuclear matter at $T = 6$ MeV. The lightest clusters now dominate up to about 0.025 fm^{-3} while, in contrast, the abundance of the heaviest clusters $51 \leqslant A \leqslant 61$ becomes negligibly small for all densities at this temperature as well as at higher temperatures as will be seen in the following figures. Now the intermediate mass fragments $11 \leqslant A \leqslant 40$ dominate the scene at the higher densities $\rho > 0.025$ nucleons fm^{-3}. This can be understood by noting that at this relatively high temperature the heaviest clusters are not stable and undergo multifragmentation. Thus at $T = 6$ MeV the intermediate mass fragments dominate the scene especially at the higher

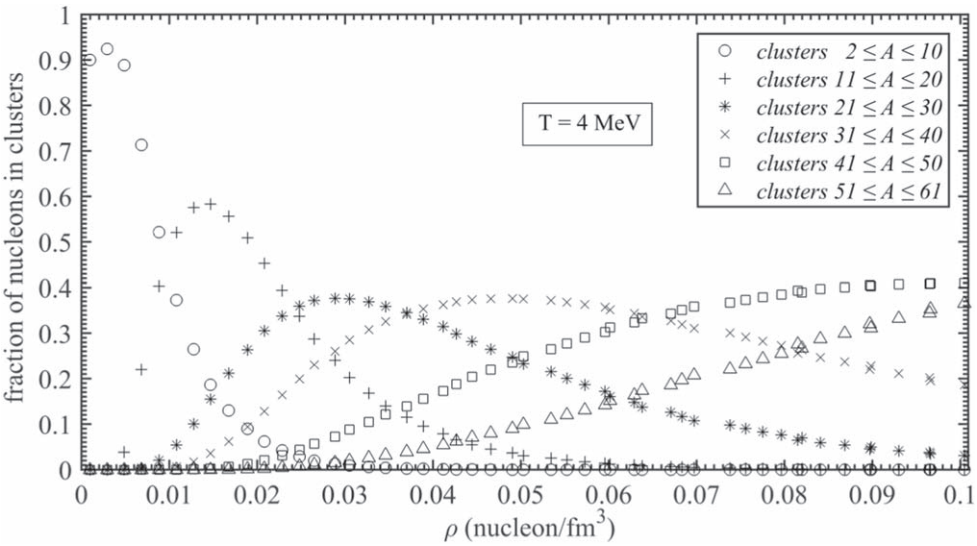

Figure 3. Cluster abundances at $T = 4$ MeV as a function of the total density.

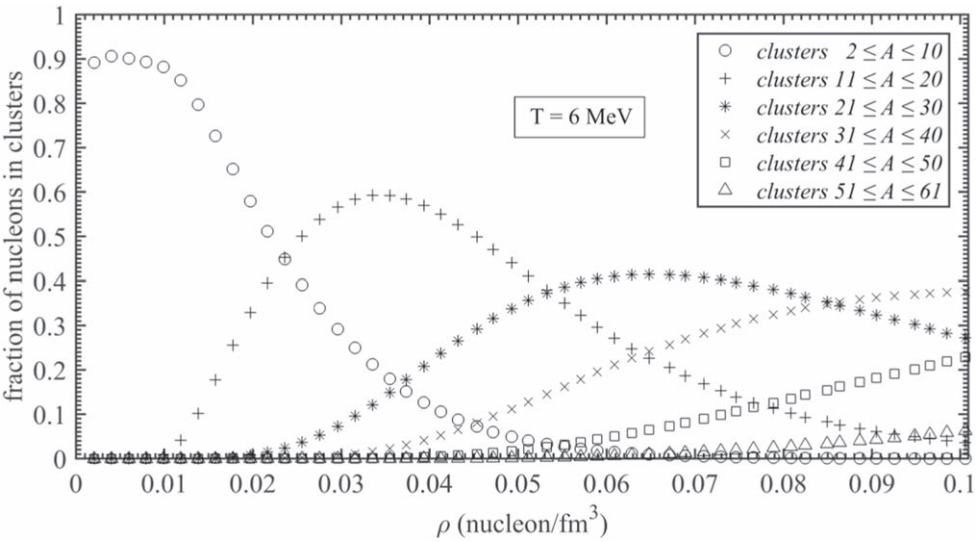

Figure 4. Cluster abundances at $T = 6$ MeV as a function of the total density.

densities. This dominance of the intermediate mass fragments at intermediate densities has been observed experimentally [10] and has been predicted theoretically in the statistical multifragmentation models [11–14]. The temperature $T = 6$ MeV is close to the limiting temperature predicted for heavy nuclei [6, 19, 20]. The limiting temperature is the highest temperature at which a hot heavy nucleus can survive while in equilibrium with the surrounding vapour.

The same trends continue as we go to higher temperatures with the heavier fragments becoming less and less abundant as the temperature is increased as can be seen from figures 5,

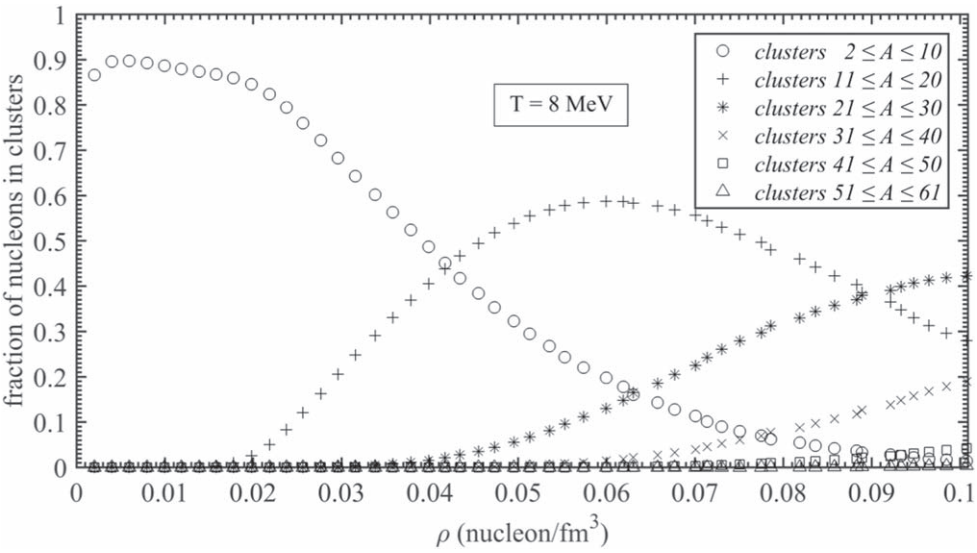

Figure 5. Cluster abundances at $T = 8$ MeV as a function of the total density.

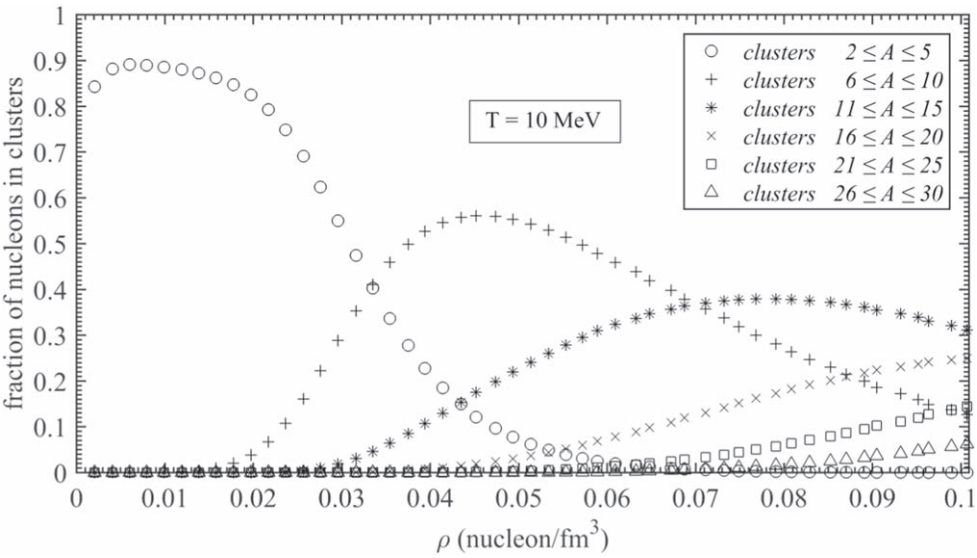

Figure 6. Cluster abundances at $T = 10$ MeV as a function of the total density.

6 and 7 for temperatures $T = 8$, 10 and 12 MeV, respectively. Within the liquid–gas phase transition picture increasing the temperature means that the nuclear system is getting closer to the critical temperature (which is found to be 12.5 MeV as described in the following section). Above the critical temperature only a single gaseous phase exists and the large liquid drops disappear. Therefore as the system gets closer to the critical temperature the average mass of the fragments becomes smaller and we have complete vapourization above the critical temperature. It can be seen that at $T = 8$ MeV the abundance of clusters with $A > 40$ is

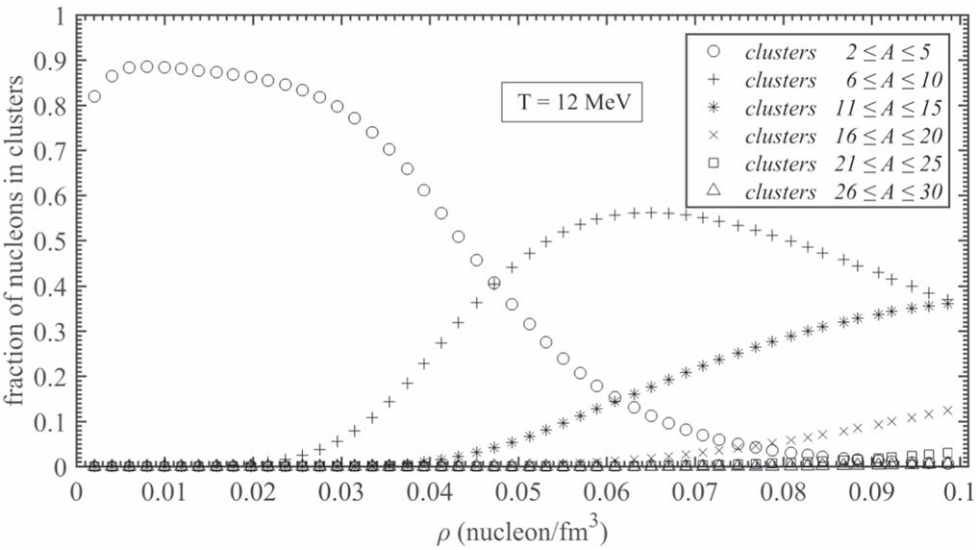

Figure 7. Cluster abundances at $T = 12$ MeV as a function of the total density.

completely negligible while at $T = 10$ MeV the abundance of clusters with $A > 30$ is negligibly small. Similarly at $T = 12$ MeV even clusters with $A > 20$ have a vanishingly small presence. Note that in figures 6 and 7 we have used smaller cluster size groups (groups of 5 rather than 10 cluster sizes) since the abundance of clusters with $A > 30$ is negligibly small.

4. The equation of state of nuclear matter and the critical temperature

In the present section we evaluate the equation of state of nuclear matter within the modified NSE model and then calculate the critical temperature of infinite nuclear matter. This approach has the advantage that it does not depend on any particular effective nuclear interaction as the nucleons interact only through the formation of clusters. It also does not make the assumption of a uniform density but includes clusters (or fragments) of various sizes and would therefore be relevant in the mechanically unstable region lying between the low density gas or vapour phase and the high-density liquid phase. This unphysical mechanical instability results from the assumption of a uniform density which leads to unphysical oscillations in the pressure isotherms in the gas–liquid transition region. The critical temperature is the lowest temperature at which the unphysical oscillations in the isotherms disappear and the critical point is determined by the merging of the maximum and minimum of the isotherms and the simultaneous vanishing of $\frac{\partial P}{\partial \rho}$ and $\frac{\partial^2 P}{\partial \rho^2}$. Abandoning the concept of a uniform density is particularly relevant near the critical point where the fluid fluctuates wildly and the concept of a uniform density definitely breaks down.

In the present model the pressure of nuclear matter is the sum of the partial pressures of the free nucleons and the various clusters:

$$P = P_{\text{free}} + \sum_C P_C, \tag{8}$$

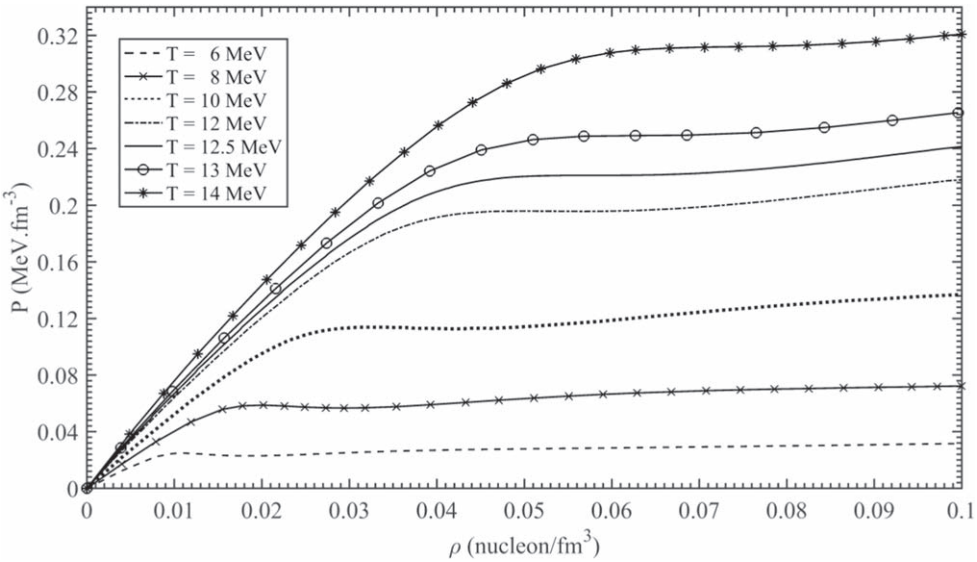

Figure 8. Pressure isotherms for various temperatures below and above the critical temperature.

where the partial pressure of the free nucleons is given by that of an ideal Fermi gas of nucleons

$$P_{\text{free}} = P_{\text{id}}(T,\ \rho_{\text{free}}) = T\rho_{\text{free}}\left[1 + \sum_{n=1}^{\infty} b_n \left[\frac{\lambda_T^3 \rho_{\text{free}}}{g}\right]^n\right]. \tag{9}$$

Equation (9) was derived [6, 21] along the same lines as equation (2) for the chemical potential of an ideal Fermi gas, and the b_n coefficients are the same as those in equation (2). The partial pressure of a fermionic cluster is also calculated with an equation similar to equation (9) but at a cluster density ρ_C given by equation (3) and with the degeneracy factor $g = 2s + 1$ where s is the ground state spin of the corresponding isolated nucleus. For bosonic clusters the partial pressure is calculated from the pressure of an ideal Bose gas which is given by an equation similar to equation (9) except that the b_n coefficients are replaced by the a_n coefficients where

$$a_n = (-1)^n b_n.$$

The total pressure is then calculated by summing all the partial pressures as in equation (8) and the total density is calculated from the partial densities as in equation (6). The resulting total pressure versus total density isotherms are plotted in figure 8 for a few temperatures below and above the critical temperature. It is seen from figure 8 that the critical point resulting from the present model occurs at $T_c = 12.2\,\text{MeV}$, $\rho_c = 0.057$ nucleons fm^{-3} and $P_c = 0.22\,\text{MeV.fm}^{-3}$.

It is noted that the critical temperature obtained in the current model is much less than the values obtained from the usual equations of state such as those employing a nucleon–nucleon interaction of the Skyrme type. These equations lead to critical temperatures that range from about 17.3 MeV for soft equations of state to 22.9 MeV for hard equations of state [6, 19, 20]. This is also in agreement with previous predictions that clustering leads to a reduction in the critical temperature [1]. It is also seen from figure 8 that the unphysical oscillations in the

isotherms below the critical temperature are much less than the oscillations that occur in the usual equations of state which assume a uniform density and lead to van der Waal type oscillations in the isotherms. This is because the present model assumes the existence of clusters of various sizes and does not invoke the unphysical concept of a uniform density.

5. Cluster multiplicity and its derivatives

Recent investigations [25–27] have indicated that the occurrence of a maximum in the multiplicity derivative $\frac{dM}{dT}$ in heavy ion collisions is an indication of the first order liquid–gas phase transition. In [25, 26] the multiplicity derivative was evaluated in the canonical thermodynamic model and was found to have a maximum near $T = 5$ MeV. The multiplicity derivative was also evaluated in the lattice gas model at a density of about $1/6$ nuclear saturation density and was found to have a maximum near $T = 4$ MeV. In [27] the multiplicity derivative was also evaluated at a density of about $1/6$ nuclear saturation density with the use of the statistical multifragmentation model [11–14] and the maximum was found to occur at $T = 5.3$ MeV. It would be interesting to see if the present model can produce a similar result.

In the present model we evaluate the multiplicity M for a system of 300 nucleons. For a given density and a given temperature, the cluster abundances determined in section 3 are used to calculate the multiplicity (approximated to the nearest integer) for each cluster type and then the total multiplicity for the desired density is plotted as a function of temperature. The derivative $\frac{dM}{dT}$ is then evaluated and the results are shown in figure 9 for four different values of the total density.

At the lowest density $\rho = 0.01$ nucleons fm^{-3} a single maximum appears at a temperature of about 6 MeV which is roughly in agreement with the earlier predictions [25–27]. However at higher densities this peak moves to lower temperatures and a second peak appears at higher temperatures. This second peak occurs at about $T = 8$ MeV for $\rho = 0.02$ nucleons fm^{-3} then shifts to about $T = 10$ MeV for $\rho = 0.03$ nucleons fm^{-3} and finally shifts to about $T = 12$ MeV at the highest density considered $\rho = 0.04$ nucleons fm^{-3}.

Our interpretation is that the first peak is related to the occurrence of the liquid–gas phase transition at the densities considered while the second peak is a remnant of the second-order phase transition at the critical point, The second peak is not relevant to finite systems which cannot survive above the limiting temperature [19, 20] as mentioned above in the introduction. It must be recalled that the present work assumes that the Coulomb force is turned off so that the second peak is a reflection of a phase transition in a hypothetical infinite system. It is therefore the first peak that is relevant for finite systems and it is interesting that it appears in the expected density and temperature ranges. This is because the liquid–gas phase transition is essentially determined by the nuclear force and so can survive in a finite system, while the limiting temperature is determined by the Coulomb force [19, 20].

In conclusion, we have calculated cluster abundances in low and intermediate density nuclear matter at temperatures in the range 2–12 MeV using a modified version of the NSE model. At low temperatures light clusters (mainly alphas at $T = 2$ MeV and deuterons at $T \geqslant 4$MeV) dominate at low densities while the heavier clusters dominate at increasingly higher densities. As the temperature increases the abundance of the light clusters increases and extends to higher densities at the expense of the heavier clusters. Whereas it is found at $T = 2$ MeV that 80% of the bound nucleons at the highest density considered come from the group with the heaviest clusters $51 \leqslant A \leqslant 61$ the corresponding abundance drops to 35% at $T = 4$ MeV, then drops further to 5% at $T = 6$ MeV and finally becomes vanishingly small at

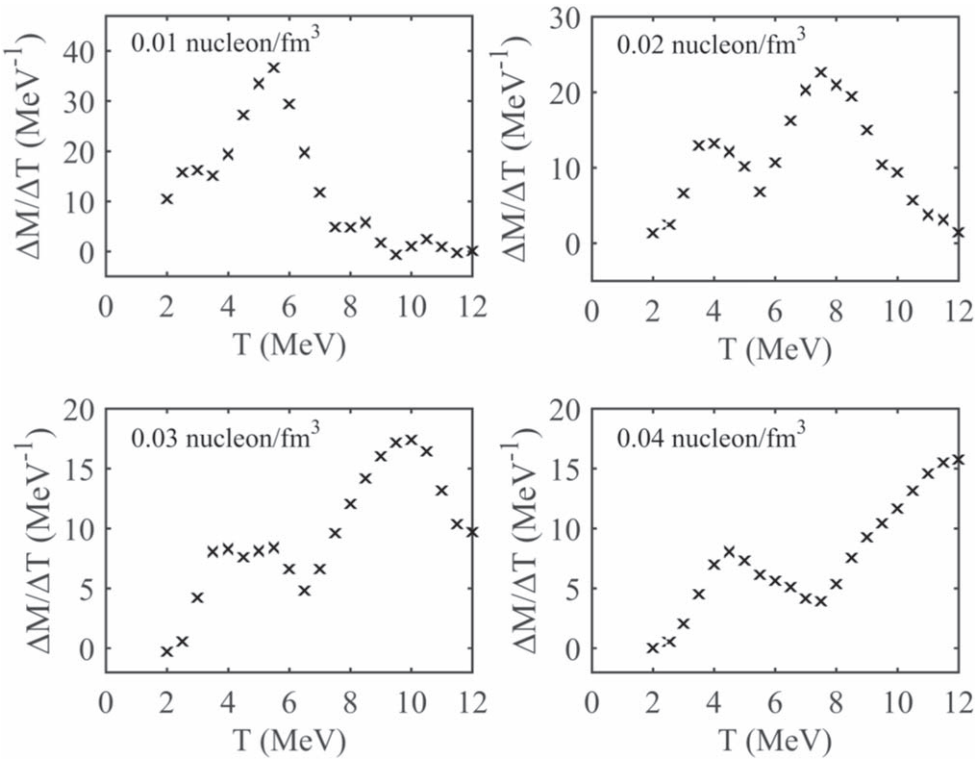

Figure 9. The multiplicity $\frac{dM}{dT}$ derivative at various densities.

$T = 8$ MeV. At $T = 10$ MeV only clusters with $A \leqslant 30$ survive while at $T = 12$ MeV only clusters with $A \leqslant 20$ are present. These results are in agreement with the coexistence of the liquid and gas phases at low temperatures and the gradual disappearance of the liquid phase (i.e. the heavy clusters) as the temperature is increased until we have complete vaporization above the critical temperature.

Using the same model, we have also evaluated the equation of state of nuclear matter and determined the critical temperature which is found to be significantly lower than that predicted by the usual equations of state obtained by ignoring the formation of clusters and assuming a uniform distribution of nucleons interacting by a two-body effective force like the Skyrme force. These latter equations together with the implied unphysical assumption of a uniform density always lead to van der Waals-like oscillations in the resulting isotherms with an unphysical mechanically unstable region between the gas and liquid phases. In addition to not depending on the particulars of any effective interaction, our equation of state leads to much smaller oscillations in the isotherms. Our equation of state is therefore very close to the true equation of state where the pressure is a steadily increasing function of the density (when the pressure on a system increases its density should increase).

Finally we have evaluated the cluster multiplicity at various densities and found that its derivative with respect to temperature has a maximum at the expected temperatures corresponding to the liquid–gas phase transition at these densities, in agreement with the results obtained from other models.

ORCID iDs

H R Jaqaman https://orcid.org/0000-0002-0812-3086

References

[1] Röpke G, Münchow L and Schulz H 1982 *Nucl. Phys.* A **379** 536
Röpke G, Schmidt M, Münchow L and Schulz H 1983 *Nucl. Phys.* A **399** 587
[2] Horowitz C J and Schwenk A 2006 *Nucl. Phys.* A **776** 55
[3] Typel S, Röpke G, Klähn T, Blaschke D and Wolter H H 2010 *Phys. Rev.* C **81** 015803
[4] Jaqaman H R 1988 *Phys. Rev.* C **38** 1418
[5] Takemoto H *et al* 2004 *Phys. Rev.* C **69** 035802
[6] Talahmeh S and Jaqaman H R 2013 *J Phys. G: Nucl. Part. Phys.* **40** 015103
[7] Kowalski S *et al* 2007 *Phys. Rev.* C **75** 014601
[8] Natowitz B *et al* 2010 *Phys. Rev. Lett.* **104** 202501
[9] Röpke G 2009 *Phys. Rev.* C **79** 014002
[10] Schüttauf A *et al* 1996 *Nucl. Phys.* A **607** 457
[11] Bondorf J 1982 *Nucl. Phys.* A **387** 25c
[12] Randrup J and Koonin S E 1981 *Nucl. Phys.* A **356** 223
[13] Gross D H E, Satpathy L, Meng T-chung and Satpathy M 1982 *Z. Phys.* **309** 41
Gross D H E 1997 *Phys. Rep.* **279** 119
[14] Bondorf J P, Botvina A S, Iljinov A S, Mishustin I N and Sneppen K 1995 *Phys. Rep.* **257** 133
[15] Clifford F and Tayler R 1965 *Mm. Ro. Astr. Soc.* **69** 21
[16] Mekjian A Z 1978 *Phys. Rev.* C **17** 1051
[17] Beyer M, Strauss S, Schuck P and Sofianos S A 2004 *Eur. Phys. J.* **22** 261
[18] Samaddar S K and De J N 2011 *Phys. Rev.* C **83** 055802
[19] Levit S and Bonche P 1985 *Nucl. Phys.* A **437** 426
[20] Jaqaman H R 1989 *Phys. Rev.* C **39** 169
[21] Jaqaman H R, Mekjian A Z and Zamick L 1984 *Phys. Rev.* C **29** 2067
[22] Typel S 2013 *J Phys.: Conf. Ser.* **420** 012078
[23] Hagel K *et al* 2012 *Phys. Rev. Lett.* **108** 062702
[24] Röpke G 2011 *Nucl. Phys.* A **867** 66
[25] Mallik S, Chaudhuri P and Das Gupta S 2017 *Phys. Rev.* C **95** 061601
[26] Das Gupta S, Mallik S and Chaudhuri P 2018 *Phys. Rev.* C **97** 044605
[27] Lin W, Ren P, Zheng H, Liu X, Huang M, Wada R and Qu G 2018 *Phys. Rev.* C **97** 054615